Clinical Imaging 53 (2019) 162–168

Contents lists available at ScienceDirect

Clinical Imaging

journal homepage: www.elsevier.com/locate/clinimag

Neuroradiology

Coronal oblique orientation of the neural foramen improves cervical spine MRI: A comparison of the sensitivity of different angulations

Wolfgang Freund[a,b,*], Frank Weber[e], Gero Hoepner[a], Reinhard Meier[a,f], Stephan Klessinger[c,d]

[a] *Diagnostic and Interventional Radiology, University Hospitals, 89081 Ulm, Germany*
[b] *Private Practice, Waaghausstr. 9, 88400 Biberach, Germany*
[c] *Neurosurgery, University Hospitals, Albert-Einstein-Allee 23, 89081 Ulm, Germany*
[d] *Neurosurgery, Nova Clinic, Eichendorfweg 5, 88400 Biberach, Germany*
[e] *German Air Force Center of Aerospace Medicine, 82256 Fuerstenfeldbruck, Germany*
[f] *Diagnostic and Interventional Radiology, Isar Clinic, Munich, Germany*

ARTICLE INFO

Keywords:
MRI
Cervical spine
Neural foramen
Radicular
Coronal oblique

ABSTRACT

Objective: Angulated projections are used in radiography to show the cervical neural foramen. Imaging the coronal oblique planes in an MRI of the cervical spine should therefore improve visualization of neural foramen pathology. This has to be demonstrated.

Patients and methods: A multi-center investigation of 40 patients with monoradiculopathy and 10 healthy controls was undertaken. T2-weighted sagittal, coronal oblique and axial slices were individually and separately examined by four readers blinded to the diagnosis. The statistical evaluation compared against the clinical gold standard of the neurological diagnosis of a single nerve root irritation or lesion.

Results: The sensitivity/specificity required to detect the relevant neural foramen pathology was 0.47/0.60 for axial, 0.57/0.90 for sagittal and 0.55/0.70 for coronal oblique scans. The readers felt significantly more confident in attributing the cause of pathology using coronal oblique planes. Interreader reliability was moderate to substantial, with the highest values for the sagittal planes (0.39–0.76) and lower values for the transversal and coronal oblique planes (0.15–0.63). Intrareader reliability was substantial, with values between 0.53 and 0.88. Reading the axial planes was significantly more time consuming than reading the other planes.

Conclusion: The use of coronal oblique planes in cervical spine MRIs increases sensitivity and confidence in attributing the cause of neural foramen obstruction. They are easy to interpret and demand less reading time than axial planes, and so the inclusion of coronal oblique planes in the workup of cervical spine MRI is recommended, at least when neural foramen pathology is suspected.

1. Introduction

Radicular symptoms like cervicobrachialgia or radiculopathic weakness of the arm are common [1] and may be caused by inflammatory or mechanical irritation of the cervical nerve roots [2–4]. Since the symptoms are often due to uncovertebral arthrosis or intervertebral disc protrusion, the proper visualization of the neural foramen is paramount [5]. Disc protrusions are reportedly the main cause of cervical radiculopathy in younger people [6], while osseous neural foramen narrowing is the leading cause in older patients [7,8].

The clinical diagnosis of cervical nerve root impingement is achieved using the Spurling maneuver [9] (tilting the head to the ipsilateral side while turning it backwards), resulting in neural foramen narrowing, which has recently been demonstrated in radiographic 3D analysis [5].

Since the nerve roots leave the cervical spinal canal via the angulated neural foramina at approximately 45° [10], they are poorly visualized on orthogonal planes. In plain radiography of the cervical spine, bilateral oblique views are standard [11] when the neural foramen is of interest, but these angulations are not generally used in magnetic resonance imaging (MRI) [12,13].

There are reports on the utility of angulated planes or 3D reformatting to better visualize neural foramen pathology [10,14–20], however this technique has not been included in the pertaining guidelines [12].

Improved visualization of neural foramen pathology is useful, however, especially preoperatively, to discern the degree and the cause (osseous or soft) of neural foramen stenosis. Preliminary tests of coronal

* Corresponding author at: Diagnostische und Interventionelle Radiologie, Universitätskliniken Ulm, Albert-Einstein-Allee 23, 89081 Ulm, Germany.
E-mail address: wolfgang.freund@uni-ulm.de (W. Freund).

https://doi.org/10.1016/j.clinimag.2018.10.011
Received 11 June 2018; Received in revised form 8 October 2018; Accepted 12 October 2018
0899-7071/

oblique slices showed promising results in 25 patients of an outpatient clinic (referenced below as Center 1) [21]. Recent reports on the MRI imaging of neural foramen stenosis also showed strong results in the coronal oblique angulations [22–26], but no report has included both normal controls and the demanding task of discerning the exact location of the symptomatic stenosis.

It was therefore hypothesized that it is useful to add coronal oblique slices to the MRI of the cervical spine. To test the diagnostic accuracy of the "new" sequence, we performed a multi-center evaluation on 40 patients and 10 controls against a clinical gold standard.

2. Patients and methods

This study adhered to the STARD 2015 (Appendix A) guidelines for reporting diagnostic accuracy studies.

2.1. Subjects

At the beginning of the study, only Center 1 (a private practice in Biberach, Germany) had experience with coronal oblique planes. With the approval of our ethics committee, the imaging technique was established in two other imaging centers (University Hospitals Ulm, Germany and the Armed Forces Hospital, Ulm, Germany). Because of the inclusion of the retrospective cases, it was decided that Center 1 should only participate with normal controls in the generation of prospective cases to exclude overrepresentation of patients from that center. Four of the 25 retrospective cases were excluded due to poor image quality. Subjects from the two other sites were included prospectively until the planned study cohort of 40 patients and 10 controls was complete (see flowchart in Fig. 1).

2.2. Inclusion criterion

The inclusion criterion was a cervical mononeuropathy (neurological diagnosis of monoradicular irritation or lesion, also used as the reference standard) in conjunction with a referral to the MRI examination. The 10 healthy controls were included consecutively from all sites, and inclusion criteria were the absence of radicular symptoms and a normal appearing MRI of the cervical spine which had been indicated to rule out cervical pathology.

2.3. Reference and reading

The reference/gold standard for mononeuropathy was defined as the neurological diagnosis of pain or weakness attributed to a single cervical nerve root. This diagnosis was made on clinical grounds – the experimental reading of the MRI took place later in a blinded fashion, so that informational contamination was ruled out.

T2-weighted sagittal, coronal oblique and axial slices were anonymized, generating 150 "series" consisting of only one spatial orientation. To prevent informational contamination from other slice orientations, no real localizers from the patients were used, but instead schematic drawings without pathology. The experimental reading took place in the presence of one author (GH), who took the time measurements and checked completeness of data. Reading time was taken on each individual rating, so that the time needed for different planes could be computed. Four readers (all senior fellows: two radiologists specialized in Musculoskeletal Radiology/Neuroradiology, one Head of Neurology and one senior neurosurgeon, each with > 10 years of experience reading spine MRIs), individually read the cases, blinded to the diagnosis and the results of the other readers. Two were experienced with coronal oblique slices; the others received 10 min of training. Criteria were reading time, level and side, as well as the cause and grading of the neural foramen stenosis and the subjective level of

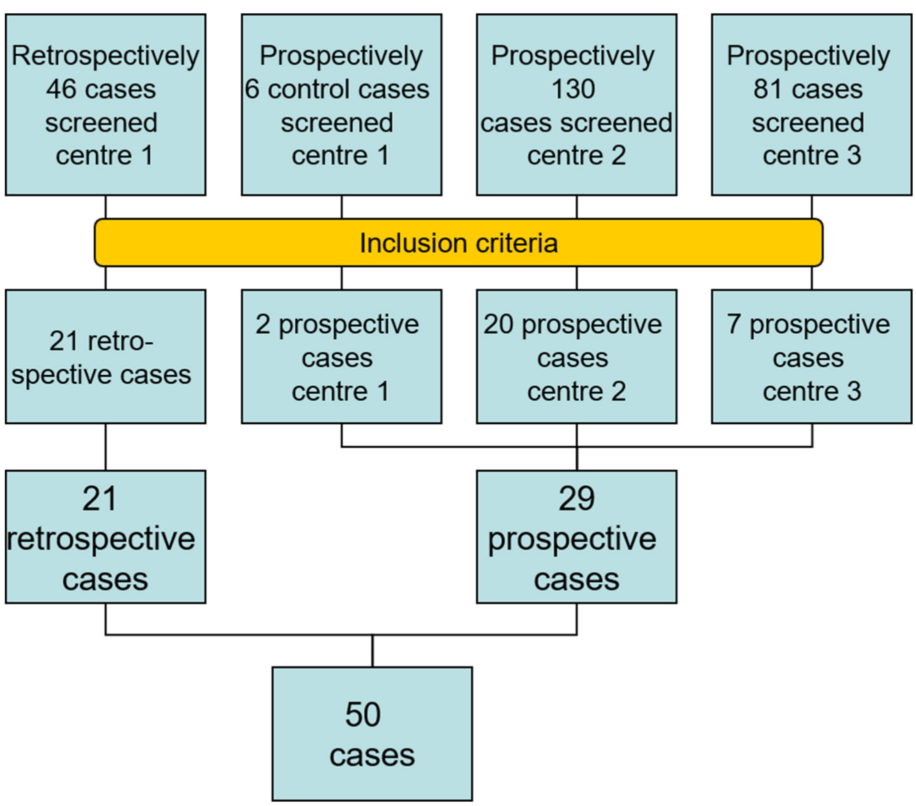

Fig. 1. Flowchart of subject inclusion of the 50 cases. The retrospective cases had been established beforehand. The 50 cases were included as planned. One case of violation of the inclusion criteria was detected and replaced with a case from the retrospective reserve.

confidence on a 100-point visual analogue scale (VAS). We were able to compare the results of two readers with data from the previous preliminary study [21] (intrarater agreement) and computed interrater agreement for all four readers.

Since we were not interested in the performance of individual readers but rather in the performance of the different angulations, we decided to aggregate the data of the four readers when comparing the angulations. Data from the individual readers was aggregated to form an averaged blinded reader [27]. The congruence of at least three of the four raters was necessary to reach agreement for qualitative variables, and the arithmetic mean was calculated for quantitative variables.

This aggregated data (averaged blinded reader) can be used to further calculate sensitivity and specificity of single slice orientations against the clinical gold standard, but it can also be used to calculate the combined sensitivity and specificity of any combination of slice orientations. In clinical routine, for example, sagittal and axial orientations are used. We wanted to test whether the exchange of one orientation with the "new" coronal oblique or the addition of the coronal oblique orientation would increase the sensitivity or specificity of the diagnostic procedure. This necessitated the definition of a combined sensitivity or specificity. Here we followed the clinical routine of parallel testing [28] and defined the *combined sensitivity* as the ratio of cases detected in at least one orientation divided by the number of positive cases (the "or rule" as described by Weinstein et al. [28]). This measure would increase with each addition of an extra slice orientation.

The *combined specificity* according to the "or rule" [28] is computed as the ratio of cases deemed negative in all orientations divided by true negative controls. The combined specificity will therefore decrease with the addition of orientations.

2.4. Sample size

Sample size was calculated from previous experience: a published report [21] could demonstrate a 50% higher sensitivity of the coronal oblique and sagittal orientations over the axial planes. A sample size of 50 would thus result in 80% power with p = 0.05. Comparing sagittal and coronal oblique orientations with a roughly 10% relative difference in sensitivity would require a sample of over 900 cases, a number not feasible in an experimental reading setting.

2.5. Scanners and sequences used

Scanning was performed with different MR-scanners (Magnetom Harmony 1.0 T, Avanto 1.5 T and Skyra 3 T, Siemens, Erlangen, Germany), and the sequence parameters are listed in Table 1. The planning of coronal oblique scans is illustrated in Fig. 2. Exemplary sagittal (Fig. 3), axial (Fig. 4) and coronal oblique (Fig. 5) scans are shown.

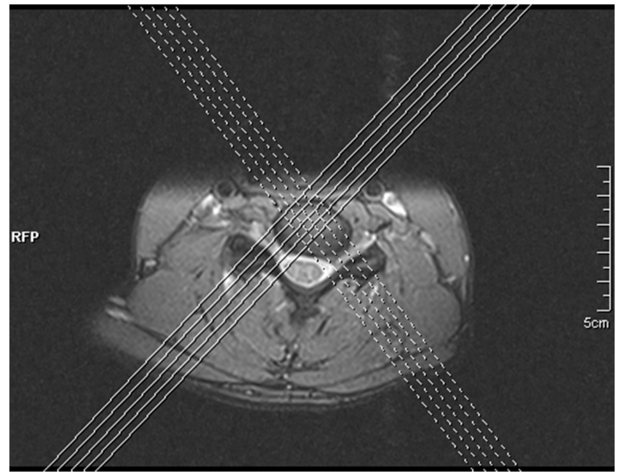

Fig. 2. Illustration of the angulation for coronal oblique scans. N.B: The scans should be planned at the level of suspected pathology to ensure perfect coverage of the neuroforamina.

2.6. Statistical analysis

Descriptive statistical analysis was performed with Microsoft Excel, and further analysis was performed using "R" version 3.2.3, from the R Foundation for Statistical Computing, 2015 [29]. *t*-Tests were performed and Cohen's kappa was computed. Results were seen as significant when p was < 0.05.

3. Results

3.1. Patients group description

The flowchart in Fig. 1 describes the selection process leading to the study population of 50 subjects (see flowchart Fig. 1). The retrospective cases had been imaged between October 2011 and September 2012. The prospective phase took place between October 2013 and July 2015. In Centers 2(3) respectively, 130(81) cases were screened, but the following numbers had to be excluded due to missing data concerning neurological status in 66(72) cases, neurological symptoms not fitting the inclusion criteria in 28(2) cases, inadequate image acquisition in 7(1) cases or inconclusive radiological data in 11(0) cases. Thus, 21(6) cases could be included.

The 50 subjects comprised 27 males and 23 females, the average age was 46.4 years (standard deviation 14.8 years). The symptomatology was recorded prior to MR-scanning (not graded according to severity) and referred to the following roots: C5: 0 cases, C6: 26 cases, C7: 12 cases, C8: 2 cases. Twenty-four cases had their symptomatic lesion on the left side, 16 on the right side. The 10 controls were asymptomatic,

Table 1
Scan parameters of the sequences used.

	Siemens Harmony 1 T			Siemens Avanto 1.5 T			Siemens Skyra 3 T		
Orientation	cor	sag	tra	cor	sag	tra	cor	sag	tra
Sequence	T2 tse	T2 tse	T2 MEDIC	T2 tse	T2 tse	T2 MEDIC	T2 tse	T2 tse	T2 MEDIC
TR	3280–3870	3000–4830	894–901	3110	3500	854	4000	5600	737
TE	106–112	105–106	22–27	106	82	24	89	89	17
Slice no	10–12	11–15	15–19	10	13–15	12	14	15	15
s thickn	3	3	3	3	3	3	3	3	3
FA	150–180	170–180	30	170	150	30	150	150	30
FOV	280–310	280–310	220–280	280	250	157 * 210	280	280	180
Resolution	320–448	348–448	256	384	384	384	512	512	384
NAQ	3–4	3–4	2	3	2	2	2	2	2

Parameters: TR: repetition time in ms, TE: echo time in ms, slice no: number of slices, s thickn: slice thickness, FA: flip angle in degrees, FOV: field of view in mm, resolution: in pixels, NAQ: number of acquisitions.

Fig. 3. A 53-year-old male with neurologically diagnosed (clinical gold standard) mononeuropathy of left C6. The neuroforaminal narrowing is ill defined on the shown sagittal T2 weighted slices. The corresponding axial and coronal oblique orientations are shown in Figs. 4 and 5.

according to the inclusion criteria.

3.2. Reading data

The reading data of the four readers was evaluated individually. The data was then aggregated to create an averaged blinded reader. This data is presented in Table 2.

There were significant differences between slice orientations in the subjective certainty of the readers: they were significantly more certain in their ratings on coronal or sagittal (turbo spin echo T2) than axial (T2 MEDIC) slices when discerning the side or level of the symptomatic neural foramen. They felt significantly more confident using coronal oblique slices than using the other two orientations when measuring the stenosis or describing root impingement. They were significantly more certain on coronal oblique slices than on axial slices when attributing the cause of neural foramen stenosis.

They were also faster to read the coronal oblique and sagittal planes than the axial planes. This was shown to be significant for sagittal planes ($p = 0.004$), and barely missed significance on coronal oblique planes ($p = 0.056$). There was no significant difference regarding the results from the different scanners: correct detection rates for all readers/the averaged blinded reader showed no significant differences (Fisher test $p = 0.33/0.12$).

3.3. Comparison of different imaging angulations

The test statistics for the detection of the symptomatic neural foramen in cervical spine MRI of different scan orientations are shown in Table 3. The sensitivity and specificity of detecting the relevant neural foramen stenosis was better for (T2 turbo spin echo) sagittal and coronal oblique orientations than for the axial (T2 MEDIC) orientation.

The readers experienced with coronal oblique slices achieved higher mean sensitivity (0.68 vs. 0.55) and specificity (0.8 vs. 0.7) than inexperienced readers. Interrater reliability was higher for experienced raters (kappa 0.67) than inexperienced raters (kappa 0.35). Intrarater reliability reached kappa values of 0.53–0.88.

3.4. Combination of imaging angulations

The combination of the two commonly used orientations (axial and sagittal) increased the combined sensitivity, and the addition of the coronal oblique scans further improved it (see Table 4).

3.5. Intrarater and interrater agreement

Test-retest agreement mostly reached values of 60–80%, which can be described as substantial [30]. It was worse for axial slices and better for coronal oblique and sagittal slices (see Table 3).

Interrater agreement was highest for sagittal orientations. The agreement mostly reached 40–80%, which can be described as moderate to substantial [30]. Coronal oblique scans (as reported above) were interpreted more coherently by experienced readers.

4. Discussion

Results using the proposed coronal oblique orientations in cervical spine MRI were superior to the results using the traditionally favored axial slices in the diagnosis of neural foramen pathology.

4.1. Routine angulations in cervical spine MRI

Sagittal and axial slices are acquired in a routine diagnostic MRI. Although only these two orientations are recommended by national bodies like the American College of Radiology [12] or the Deutsche

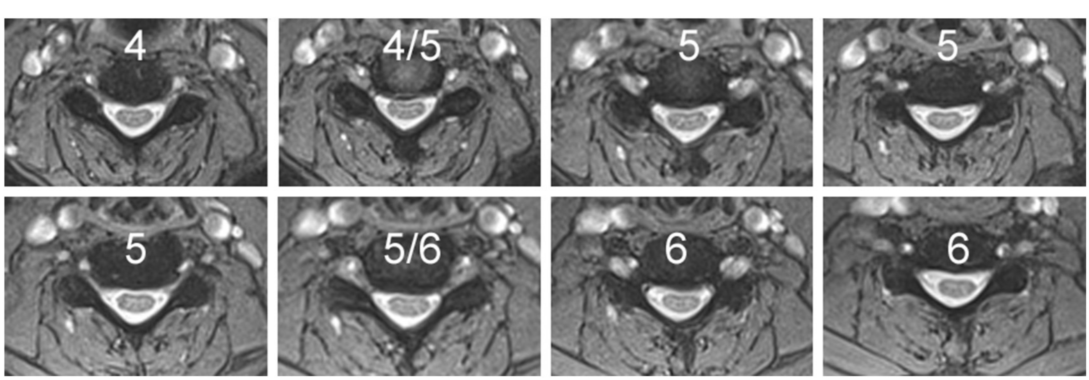

Fig. 4. The same case as in Figs. 3 and 5 (mononeuropathy of left C6). The neuroforaminal narrowing is not easily detected on the axial T2 weighted slices.

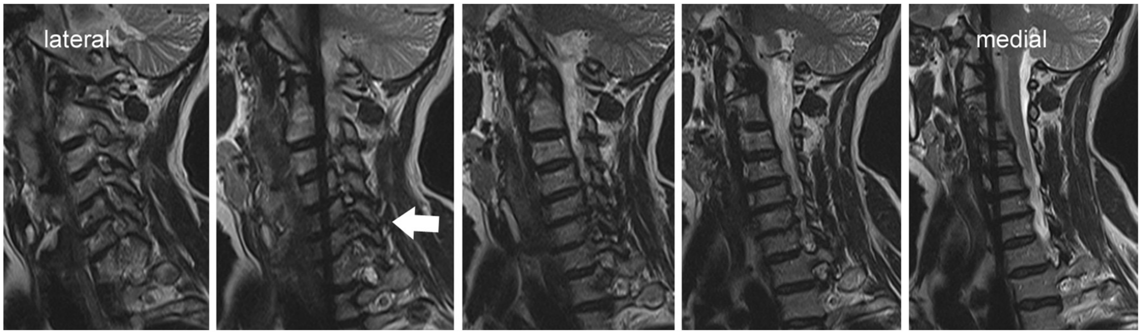

Fig. 5. The same case as in Figs. 3 and 4, experiencing mononeuropathy of left C6. The neuroforaminal narrowing is ill defined on sagittal (Fig. 3) or axial (Fig. 4) slices. However, on the left side coronal oblique scans shown here, uncovertebral exostosis with narrowing of the neural foramen is nicely captured.

Table 2
Results of the calculated averaged blinded reader concerning the measurements on the different scan orientations.

Scan orientation	S true	SCS	L true	SCL	%sten	SC%	G Root	SCG	SCC	E time
Coronal oblique	0.71	72.4	0.74	74.9	46.5	72.3	1.4	72.4	77.2	50.3
Sagittal	0.78	72.6	0.74	73.7	38.9	67.3	1.1	68.2	74.7	47.7
Axial	0.68	68.9	0.67	66.8	42.9	64.2	1.3	64.6	71.4	55.4
t-Test p for difference	0.12–0.64	0.19–0.95	0.26–0.94	< 0.01–0.66	0.09–0.43	< 0.01–0.17	0.12–0.48	< 0.01–0.12	< 0.01–0.26	< 0.01–0.33

Variables: S true: % of correctly identified laterality of the symptomatic neuroforamen. SCS: subjective certainty (VAS) concerning the side. L true: % of correctly identified levels of the symptomatic neuroforamen. SCL: subjective certainty (VAS) concerning the level. %sten: % stenosis of the neuroforamen. SC%: subjective certainty (VAS) concerning the % stenosis. GRoot: grading of the root impingement. SCG: subjective certainty concerning the GRoot. SCC: subjective certainty (VAS) concerning the cause. E time: time needed for evaluation of the scans.

Table 3
Test statistics for the detection of the symptomatic neuroforamen in cervical spine MRI of different scan orientations

Scan orientation	Sensitivity	Specificity	PPV	positive LR	negative LR	Inter-K	Intra-K
Coronal oblique	0.55 (0.38–0.71)	0.70 (0.35–0.93)	0.88 (0.69–0.97)	1.83 (0.68–4.92)	0.64 (0.38–1.09)	0.15–0.62	0.53–0.88
Sagittal	0.57 (0.41–0.73)	0.90 (0.55–1.00)	0.96 (0.79–1.00)	5.75 (0.88–37.62)	0.47 (0.31–0.72)	0.39–0.76	0.67–0.86
Axial	0.47 (0.32–0.64)	0.60 (0.26–0.88)	0.83 (0.61–0.95)	1.19 (0.52–2.71)	0.88 (0.49–1.57)	0.23–0.63	0.61–0.71

Abbreviations: PPV: positive predictive value. Inter-K: interreader kappa (ratings 2015). Intra-K: intrareader kappa (comparison between ratings 2013 and 2015). Results are given with 95% confidence intervals (in brackets).

Table 4
Test statistics of combinations of different scan orientations for the detection of the symptomatic neuroforamen in cervical spine MRI.

Scan orientation	Sensitivity	Specificity	PPV	positive LR	negative LR
Sagittal + axial	0.65 (0.48–0.79)	0.4 (0.12–0.74)	0.81 (0.64–0.93)	1.08 (0.62–1.89)	0.87 (0.37–2.09)
Sagittal + coronal oblique	0.62 (0.46–0.77)	0.6 (0.26–0.88)	0.86 (0.68–0.96)	1.56 (0.70–3.46)	0.62 (0.33–1.19)
Sagittal + axial + coronal oblique	0.68 (0.51–0.81)	0.2 (0.03–0.56)	0.77 (0.60–0.90)	0.84 0.58–1.23)	1.62 (0.44–6.07)

Abbreviations: PPV: positive predictive value. Sensitivity (If at least one detects correctly). Specificity (If all agree correctly). Results are given with 95% confidence intervals (in brackets).

Röntgengesellschaft [13], we think that the addition of coronal oblique slices supports the diagnostic process, as has been shown by our data. When considering sensitivity and specificity for a single orientation, the coronal oblique slices were nearly as accurate as the sagittal planes (T2 turbo spin echo each), and were significantly better than the axial planes (T2 MEDIC). In clinical routine, however, a combination of sagittal and axial planes is used. In the context of our study, the combination of sagittal and coronal oblique scans would yield nominally better test results (especially higher specificity for the diagnosis of neural foramen pathology). The combination of all three planes further increases sensitivity – at the cost of specificity. Nevertheless, coronal oblique angulations have been included in the routine protocols in our institutions, and the referring neurosurgeons demand them.

On first sight, our results seem worse than the excellent values found in other reports [19,24,25]. This difference, however, may be attributed to the fact that our inclusion criteria were clinical (mononeuropathy), while, for example, Shim et al. [19] included only cases with a clear symptomatology and matching MRI. It is also more demanding to perform against a clinical gold standard and against normal controls, and to name the side and level of the relevant pathology rather than simply grading the maximal stenosis or any pathology.

We suppose that the small but incremental benefit of adding sequences to increase the sensitivity may correspond well with clinical routine. Moreover, if you are interested in neural foramen pathology, it makes sense to choose the perfect angulation to visualize the neural foramen, however it is of interest that the combined specificity as defined above is reduced by each addition to the diagnostic protocol. The normally used combination of axial and sagittal planes is worse than the combination of sagittal and coronal planes. When using the measures of likelihood ratios LR+ and LR− (see Table 3), it would be preferable to use only the sagittal plane or a combination of the sagittal and coronal oblique planes. This is in contrast to the clinical routine, where neural foramen pathology is often assessed on axial planes. These axial planes demonstrated the lowest performance in our evaluation.

4.2. Subjective certainty

The subjective feeling of diagnostic certainty concerning neural foramen pathology (see Table 2) is clearly better with coronal oblique planes than other orientations. This is due to the optimal angulation of the slices and thus visualization of the neural foramen.

4.3. Kappa

Although our numbers are worse than the data reported by [32], we think that our task was much more demanding. We had to correctly identify the presence and locus of a symptomatic neural foramen against a clinical gold standard (validity) instead of the criterion used by Park et al., where similarity of reporting was counted (reliability, irrespective of a gold standard). The observed interrater reliability differs between angulations with the most robust reliability for sagittal planes, ranging from moderate to substantial [30], however, it is only poor-to-substantial for axial or coronal oblique scans, with higher reliability among more experienced readers. Intrarater reliability is mostly substantial to excellent with no significant difference between the angulations. This is not surprising, since the more experienced readers took part in the previous study, so that the data on intrarater reliability refers to the more experienced readers.

4.4. Time considerations

The time needed to scan and to read is an important argument when choosing the appropriate diagnostic procedures. The lateral parts of the vertebral bodies and thus the neural foramen are often incompletely covered in routine sagittal slices due to scanning time constraints. Here five coronal oblique scans on each side offer improved coverage of the neural foramen with an ideal angulation of approximately 45°. These 10 slices are acquired in the same time as 10 conventional slices. The readers were able to read the coronal oblique and sagittal planes faster than the axial planes.

4.5. Technical considerations

Optimized visualization of the neural foramen depends on the angulation of the images. This can be achieved either by individually planning 2D sequences a priori, or by reformatting data from 3D. Reports show that the reconstruction of optimally angulated slices is feasible [17,20], and that some techniques may even yield higher contrast than standard sequences [33]. The application of contrast medium is necessary for some diagnostic problems, and newer sequences like DWI or DTI show promise [34–36], but the concern of this manuscript was more with the angulation per se.

Up to now, for practical reasons (mainly scan time and compensation rules) 2D sequences have been preferred in clinical routine. The proposed coronal oblique sequences are shown in Table 1, and have acquisition times similar to that of the sagittal sequences.

Since the scanner type did not significantly affect the results and the cases presented in this study had been scanned on different scanners, ranging from 1 to 3 T, and both in hospital- as well as practice-settings, the results are deemed to be generalizable.

4.6. Limitations

We used a clinical gold standard in our study: the neurological diagnosis of mononeuropathy (irritation or lesion of a single radix). This is sensible from the viewpoint of indicating the MRI, however the definitions of other studies used the neurosurgical postoperative diagnosis (and included only operated patients), thus enhancing the chance to detect a confirmed mechanical cause of the symptoms. There is the risk of circular reasoning, however, if only cases suspected first on clinical and radiological grounds are included, which secondly underwent surgery with confirmation of the clinical and radiological suspicion. This inclusion process dramatically increases the chance of "diagnostic" radiological procedures. Different etiologies were included in our sample, however, so that not only mechanical causes but also inflammation or distension of the nerve roots could be causative – neither of which are detectable by conventional MRI.

Blinding not only to clinical information but also to information contained in other planes was deemed necessary, so the use of a schematic localizer was introduced in order for the experiment to be able to assess single slice orientations without contamination by information from other orientations. The inclusion of the retrospective cases from an earlier study resulted in a mixture of both retrospective and prospective cases, but permitted the exploration of intra- as well as interreader variability.

The comparison was made using T2 turbo spin echo (sagittal and coronal oblique) and MEDIC sequences. This may account for some of the disadvantages of the transversal planes, since the visualization of anatomic detail may be better in Turbo spin echo sequences.

The sample size was calculated to permit comparisons between axial and coronal oblique planes where earlier experience had shown effect sizes of 50%. A comparison of sagittal and coronal oblique orientations is thus not sufficiently powered, however it is not the aim to abolish sagittal planes, but rather to include (perhaps in exchange with one axial plane) the "new" orientation into the workup of cervical spine MRI.

5. To conclude

We think that the proposed coronal oblique orientations can be interpreted quickly, and yield important information.

A complete diagnostic workup of neural foramen pathology is important, especially preoperatively, since the results may influence the indications for operative treatment and surgical technique. Coronal oblique planes in cervical spine MRI improve sensitivity in order to detect the laterality and level of pathology and add subjective confidence in attributing the cause of neural foramen obstruction. They are easy to interpret and show good test-retest agreement.

Acknowledgements

The cooperation and support of the radiology department of the German Armed Forces Hospital Ulm is highly appreciated. The study was investigator-driven, and no external funding was used. There are no conflicts of interest for the authors.

IRB: The Ethics committee of the University of Ulm has approved the study with the tracking number 289/12.

Appendix A. Supplementary data

Supplementary data to this article can be found online at https://doi.org/10.1016/j.clinimag.2018.10.011.

References

[1] Dillin W, Booth R, Cuckler J, Balderston R, Simeone F, Rothman R. Cervical radiculopathy. A review. Spine (Phila Pa 1976) 1986;11(10):988–91.
[2] DGN-Leitlinienkommission. Zervikale Radikulopathie. http://www.awmf.org/uploads/tx_szleitlinien/030-082l_S1_Zervikale_Radikulopathie_2012_verlaengert.pdf; 2012, Accessed date: 23 February 2016.
[3] Garfin SR, Rydevik B, Lind B, Massie J. Spinal nerve root compression. Spine (Phila Pa 1976) 1995;20(16):1810–20.
[4] Furusawa N, Baba H, Miyoshi N, Maezawa Y, Uchida K, Kokubo Y, et al. Herniation of cervical intervertebral disc: immunohistochemical examination and measurement of nitric oxide production. Spine (Phila Pa 1976) 2001;26(10):1110–6.
[5] Mao H, Driscoll SJ, Li JS, Li G, Wood KB, Cha TD. Dimensional changes of the neuroforamina in subaxial cervical spine during in vivo dynamic flexion-extension. Spine J 2016;16(4):540–6.
[6] Murphey F, Simmons JC, Brunson B. Chapter 2. Ruptured cervical discs, 1939 to 1972. Clin Neurosurg 1973;20:9–17.

[7] Yoon SH. Cervical radiculopathy. Phys Med Rehabil Clin N Am 2011;22(3):439–46. [viii].

[8] Boden SD, McCowin PR, Davis DO, Dina TS, Mark AS, Wiesel S. Abnormal magnetic-resonance scans of the cervical spine in asymptomatic subjects. A prospective investigation. J Bone Joint Surg Am 1990;72(8):1178–84.

[9] Tong HC, Haig AJ, Yamakawa K. The Spurling test and cervical radiculopathy. Spine (Phila Pa 1976) 2002;27(2):156–9.

[10] Sohn HM, You JW, Lee JY. The relationship between disc degeneration and morphologic changes in the intervertebral foramen of the cervical spine: a cadaveric MRI and CT study. J Korean Med Sci 2004;19(1):101–6.

[11] ACR. ACR-ASSR-SPR-SSR practice parameter for the performance of spine radiography. http://www.acr.org/~/media/03586F4164384C6C995E83CE68A5C835.pdf; 2012, Accessed date: 17 February 2016.

[12] ACR. ACR–ASNR–SCBT-MR practice parameter for the performance of magnetic resonance imaging (MRI) of the adult spine. http://www.acr.org/~/media/ACR/Documents/PGTS/guidelines/MRI_Adult_Spine.pdf; 2012, Accessed date: 17 February 2016.

[13] DRG. Von der AG Muskuloskelettale Diagnostik der Deutschen Röntgengesellschaft empfohlene Protokolle für MRT-Untersuchungen der Gelenke und Wirbelsäule. Fortschr Roentgenstr 2006(01):128–30.

[14] Daniels DL, Hyde JS, Kneeland JB, Jesmanowicz A, Froncisz W, Grist TM, et al. The cervical nerves and foramina: local-coil MR imaging. AJNR Am J Neuroradiol 1986;7(1):129–33.

[15] Pech P. Correlative investigations of craniospinal anatomy and pathology with computed tomography, magnetic resonance imaging and cryomicrotomy. Acta Radiol Suppl 1988;372:127–48.

[16] Yenerich DO, Haughton VM. Oblique plane MR imaging of the cervical spine. J Comput Assist Tomogr 1986;10(5):823–6.

[17] Kwon JW, Yoon YC, Choi SH. Three-dimensional isotropic T2-weighted cervical MRI at 3T: comparison with two-dimensional T2-weighted sequences. Clin Radiol 2012;67(2):106–13.

[18] Roberts CC, McDaniel NT, Krupinski EA, Erly WK. Oblique reformation in cervical spine computed tomography: a new look at an old friend. Spine (Phila Pa 1976) 2003;28(2):167–70.

[19] Shim JH, Park CK, Lee JH, Choi JW, Lee DC, Kim DH, et al. A comparison of angled sagittal MRI and conventional MRI in the diagnosis of herniated disc and stenosis in the cervical foramen. Eur Spine J 2009;18(8):1109–16.

[20] Kamogawa J, Kato O, Morizane T, Hato T. Virtual pathology of cervical radiculopathy based on 3D MR/CT fusion images: impingement, flattening or twisted condition of the compressed nerve root in three cases. Springerplus 2015;4:123.

[21] Freund W, Klessinger S, Mueller M, Halatsch ME, Hoepner G, Weber F, et al. Utility of coronal oblique slices in cervical spine MRI: improved detection of the neuroforamina. Radiologe 2015;55(11):1000–8.

[22] Fu MC, Webb ML, Buerba RA, Neway WE, Brown JE, Trivedi M, et al. Comparison of agreement of cervical spine degenerative pathology findings in magnetic resonance imaging studies. Spine J 2016;16(1):42–8.

[23] Park MS, Moon SH, Lee HM, Kim TH, Oh JK, Lee SY, et al. Diagnostic value of oblique magnetic resonance images for evaluating cervical foraminal stenosis. Spine J 2015;15(4):607–11.

[24] Kim W, Ahn KS, Kang CH, Kang WY, Yang KS. Comparison of MRI grading for cervical neural foraminal stenosis based on axial and oblique sagittal images: concordance and reliability study. Clin Imaging 2017;43:165–9.

[25] Lee JE, Park HJ, Lee SY, Lee YT, Kim YB, Lee KH, et al. Interreader reliability and clinical validity of a magnetic resonance imaging grading system for cervical foraminal stenosis. J Comput Assist Tomogr 2017;41(6):926–30.

[26] Lee KH, Park HJ, Lee SY, Chung EC, Rho MH, Shin H, et al. Comparison of two MR grading systems for correlation between grade of cervical neural foraminal stenosis and clinical manifestations. Br J Radiol 2016;89(1062):20150971.

[27] Ryan AF, Semelka RC, Molina PL, Yonkers S, Vaidean G. Evaluation of radiologist interpretive performance using blinded reads by multiple external readers. Invest Radiol 2010;45(4):211–6.

[28] Weinstein S, Obuchowski NA, Lieber ML. Clinical evaluation of diagnostic tests. AJR 2005;184(1):14–9.

[29] R_Development_Core_Team. R. A language and environment for statistical computing 3.2.3 (2015-12-10) ed. Vienna: R Foundation for Statistical Computing; 2015.

[30] Landis JR, Koch GG. The measurement of observer agreement for categorical data. Biometrics 1977;33(1):159–74.

[32] Park HJ, Kim SS, Lee SY, Park NH, Chung EC, Rho MH, et al. A practical MRI grading system for cervical foraminal stenosis based on oblique sagittal images. Br J Radiol 2013;86(1025):20120515.

[33] Ozturk A, Aygun N, Smith SA, Caffo B, Calabresi PA, Reich DS. Axial 3D gradient-echo imaging for improved multiple sclerosis lesion detection in the cervical spinal cord at 3T. Neuroradiology 2013;55(4):431–9.

[34] Razek A, Ashmalla GA. Assessment of paraspinal neurogenic tumors with diffusion-weighted MR imaging. Eur Spine J 2018;27(4):841–6.

[35] Razek A, Shabana AAE, El Saied TO, Alrefey N. Diffusion tensor imaging of mild-moderate carpal tunnel syndrome: correlation with nerve conduction study and clinical tests. Clin Rheumatol 2017;36(10):2319–24.

[36] Razek AA, Abdalla A, Fathy A, Megahed A. Apparent diffusion coefficient of the vertebral bone marrow in children with Gaucher's disease type I and III. Skeletal Radiol 2013;42(2):283–7.